Biosensors and Bioelectronics 143 (2019) 111606

Contents lists available at ScienceDirect

Biosensors and Bioelectronics

journal homepage: www.elsevier.com/locate/bios

Electrochemical detection of NOx gas based on disposable paper-based analytical device using a copper nanoparticles-modified screen-printed graphene electrode

Kingkan Pungjunun[a], Sudkate Chaiyo[a,b], Narong Praphairaksit[a], Weena Siangproh[c], Astrid Ortner[d], Kurt Kalcher[e], Orawon Chailapakul[a,f,**], Eda Mehmeti[e,*]

[a] Electrochemistry and Optical Spectroscopy Center of Excellence (EOSCE), Department of Chemistry, Faculty of Science, Chulalongkorn University, 254 Phayathai Road, Pathumwan, Bangkok, 10330, Thailand
[b] The Institute of Biotechnology and Genetic Engineering, Chulalongkorn University, Patumwan, Bangkok, 10330, Thailand
[c] Department of Chemistry, Faculty of Science, Srinakharinwirot University, Sukhumvit 23, Wattana, Bangkok, 10110, Thailand
[d] Institute of Pharmaceutical Sciences, Karl-Franzens University Graz, Schubertstrasse 1, Graz A-8010, Austria
[e] Institute of Chemistry, Karl-Franzens University, Universitätsplatz 1, Graz A-8010, Austria
[f] Nanotec-CU Center of Excellence on Food and Agriculture, Chulalongkorn University, Bangkok, 10330, Thailand

ARTICLE INFO

Keywords:
Gas sensing
Differential pulse voltammetry
Nitric oxide
Nitrogen dioxide
NOx gas

ABSTRACT

A disposable gas-sensing paper-based device (gPAD) was fabricated in origami design which integrates the gas adsorbent and the electrochemical detection zone in a single device. The gPAD for the determination of NOx gas uses a screen-printed graphene electrode modified with copper nanoparticles (CuNP/SPGE) to achieve high sensitivity and selectivity. The gPAD detects both, NO and NO_2 (as NOx) with same current responses. The measurement could be performed directly through differential pulse voltammetry (DPV) with a detection limit as low as 0.23 vppm and 0.03 vppm with exposure times of 25 min and 1 h, respectively. The reproducibility in terms of relative standard deviation was less than 5.1% (n = 7 devices) at 25, 75 and 125 vppm NO_2 and the lifetime of this device was more than 30 days. The gPAD was applied to detect NOx in air and exhaust gases from cars. In comparison with spectrophotometry, there are no significant differences between both methods using a paired *t*-test of the results on a 95% confidence level. The designed gPAD can provide a new template model for other gas sensors with features of disposability and portability for fieldwork analysis at low cost.

1. Introduction

Nowadays, nitrogen oxides (NOx) are important pollution components contributing not only to the greenhouse effect and the formation of acid rain, but at high levels they exert also an enormous impact on the health of humans, such as on the respiration system resulting in critical illnesses (Jeong et al., 2019; Song et al., 2019). NOx represents a sum of nitrogen monoxide (NO) and nitrogen dioxide (NO_2). However, NO in ambient air is of low toxicity, but is easily oxidized to NO_2 which is a potent toxic oxidant. Therefore, most frequently NOx is determined as NO_2 (Izumi et al., 2015). The maximum NOx concentration limit set by the United States Environmental Protection Agency (EPA) and the Occupational Safety and Health Administration (US) is 0.2 vppm (3.76 mg m^{-3}, at 25.0 °C and 1 atm) in ambient air and 5 vppm (3.76 g m^{-3}, at 25.0 °C and 1 atm) in gas-exposed industry (Allen et al., 2018; Hoa and El-Safty, 2011). Therefore, analytical methods to monitor the concentration of NOx gas are very important.

Convenient techniques for the determination of NOx comprise gas sensors, such as spectrophotometric (Passaretti Filho et al., 2015), chemiluminescence (Jung et al., 2017), laser-induced fluorescence (LIF) (Thornton et al., 2000) and resistive sensors (Rajesh et al., 2014; Deng et al., 2012). These techniques have some limitations including bulky instrumentation and high material costs. Recently, electrochemical sensors have rapidly gained significant attention for the determination of NOx because of advantages such as high selectivity, inexpensiveness and portability (Gomes et al., 2019; Lu, 2019). Voltammetric techniques, in particular differential pulse voltammetric (DPV), are attractive because of high sensitivity and tunable selectivity for NOx (Dumitrescu

* Corresponding author. Institute of Chemistry, Karl-Franzens University, Universitätsplatz 1, Graz A-8010, Austria.
** Corresponding author. Electrochemistry and Optical Spectroscopy Center of Excellence (EOSCE), Department of Chemistry, Faculty of Science, Chulalongkorn University, 254 Phayathai Road, Pathumwan, Bangkok, 10330, Thailand.
E-mail addresses: corawon@chula.ac.th (O. Chailapakul), eda.mehmeti@uni-graz.at (E. Mehmeti).

https://doi.org/10.1016/j.bios.2019.111606
Received 13 June 2019; Received in revised form 6 August 2019; Accepted 15 August 2019
Available online 21 August 2019
0956-5663/

et al., 2018; Brown and Schoenfisch, 2018). Many reports indicate that electrochemical devices can be miniaturized on paper-based design, so-called electrochemical paper-based analytical devices (ePAD). Such concepts are simple, low in cost, portable and include disposability (Dungchai et al., 2009; Chaiyo et al., 2018). Moreover, PAD is one of the most promising substrate material which can be applied in point-of-care diagnostic assays (Nantaphol et al., 2019), food safety assessment (Arduini et al., 2019) and environmental monitoring (Rattanarat et al., 2014). Origami (Ma et al., 2015) and rotational paper-based devices (Sun et al., 2018) generate high flexibility and simplicity for even complex analytical protocols.

Carbon electrodes, especially, screen-printed graphene electrodes (SPGEs) have been extensively employed in ePADs due to their easy fabrication, low cost, and inherence for large-scale production (Moreira et al., 2018; Panraksa et al., 2018). However, a limitation of SPGEs is some low sensitivity due to poor electron transfer. To overcome this drawback, we have developed nanoparticle-modified SPGEs because they can exhibit improved electroactive surface and good catalytic properties (Pungjunun et al., 2018; Manoj et al., 2018). Copper nanoparticle (CuNP)-modified carbon-based electrodes for the determination of NOx were reported in some studies because of the catalytic property of Cu towards the electrochemical conversion of NOx or their follow-up products (Zhang et al., 2015; Prakash et al., 2011).

In this work, we describe a novel sensitive method for quantifying NOx with a disposable gas-sensing paper-based device (gPAD). The latter was designed in a way that the analyte (NO, NO_2) is adsorbed on activated carbon and detected electrochemically with a copper nanoparticle-modified screen-printed graphene electrode (CuNP/SPGE). The two compartment zones of the gPAD consisted of (i) the NOx adsorber with activated carbon as adsorbent for gas collection because of its high surface area and micro-porous morphology (Ghouma et al., 2015; Belhachemi et al., 2014); and of (ii) the detection zone containing the CuNP/SPGE as working electrode. The whole sensor was fabricated with origami technique and presents a new strategy for low-cost, simple, disposable and portable sensor design in combination with excellent analytical performance for the detection of NOx in gaseous samples, such as air and exhaust gases from cars.

2. Experimental

2.1. Materials and reagents

Conductive inks of graphene, carbon and silver/silver chloride (Ag/AgCl) were purchased from Gwent group (Torfaen, United Kingdom). Copper(II) acetate anhydrous, copper fine powder, glacial acetic acid, sodium acetate trihydrate, potassium hydroxide, sodium hydroxide, sodium nitrite, iron(II) sulfate heptahydrate, sodium chloride, sodium oxalate, sodium sulfite, sulfuric acid (95–97%), nitric acid, sodium thiosulfate heptahydrate, potassium iodate, sodium iodide and ethyleneglycol were purchased from Merck (Darmstadt, Germany). Sodium phosphate dibasic heptahydrate and sodium phosphate monobasic monohydrate used for the preparation of phosphate buffer solution (PBS, 0.1 M) were purchased from Carl Roth (Karlsruhe, Germany). Activated carbon, sulfanilamide, N-(1-naphthyl) ethylenediamine dihydrochloride (NED), triethanolamine were purchased from Sigma-Aldrich (Buchs, Switzerland). Nitrogen and nitrous oxide were acquired from Messer (Bierbaum, Austria). All reagents used in this work were of analytical grade and were used without further purification. All the solutions were prepared using ultrapure water with a resistivity of 18 M Ω cm obtained by a cartridge purification system (Millipore, UK).

NO which was used as primary analyte in this work was prepared following the procedure described elsewhere (Suryaraman and Viswanathan, 1949). Briefly, a mixture of iron(II) sulfate heptahydrate (4.25 g), sodium chloride (4.25 g) and sodium nitrite (2.00 g) was sintered under moderate warming. The evolved gas was washed by deaerated NaOH solution (1.0 M) and collected over ultrapure water degassed with nitrogen. For experiments with NO, the pure gas was diluted with nitrogen, for studies with NO_2 it was diluted with air where oxidation occurred according to eqn (1).

$$2\ NO\ +\ O_{2(air)} \rightarrow 2\ NO_2 \quad (1)$$

2.2. Apparatus

Electrochemical analysis was performed with a potentiostat (PGSTAT 128 N, AutoLab, Metrohm, Switzerland) controlled by corresponding software (Nova 2.0). A three-electrode system was employed, including a copper nanoparticle-modified working electrode (CuNP/SPGE), a graphene ink counter electrode, and a Ag/AgCl reference electrode, all screen-printed onto the paper support.

Field emission scanning electron spectroscopy (FESEM) was done with an electron microscope at 15 kV (JSM-7001F, JEOL, U.K. Ltd., England). The energy dispersive x-ray spectra (EDS) was recorded on an INCA penta FETx3 model (Oxford Instruments plc, United Kingdom).

Surface area and pore size analyzer was performed on a BELSORP, mini-II nitrogen absorptometer (Germany). The nitrogen adsorption isotherms on materials was studied at −196 °C. The material was outgassed at 200 °C.

The accuracy of the sensor method was studied by comparing the results with those obtained from the Griess-Saltzman method using a UV–Visible spectrophotometer (Cary 50, Varian, United States) for absorbance measurements with a 1.0 cm path length quartz cuvette.

2.3. Preparation of activated carbon for NOx adsorption

Activated carbon powder (0.5 g) was mixed with a 1 M KOH solution (100 mL) and stirred for 4 h. Then the solution was filtered using a paper filter (Whatman No.1) and the residue was dried at 50 °C for 2 h (Lee et al., 2003).

2.4. Design and fabrication of the gPAD for NOx

The pattern for the paper device was created using Adobe Illustrator software (CC2019) followed by printing onto filter paper (Whatman No.1, A4 size) by a wax printer (Color Qube 8570 series, Xerox, Japan). The wax-patterned paper (wax zones are indicated in blue, Fig. S1, supplementary material) was divided into two zones; (i) the adsorption paper zone (each circle 8.0 mm in diameter) and (ii) the detection paper zone (4.0 mm in diameter for the working electrode, 8.0 mm in total) (Fig. S1, supplementary material). The wax-impregnated paper was placed into an oven at 175 °C (40 s) for accomplishing impregnation by wax penetrating trough the paper and forming a hydrophobic barrier. On the detection zone, graphene ink was printed as working and counter electrode on the substrate. Ag/AgCl ink was then screen-printed for the reference electrode (Fig. S2, supplementary material). After that, each device was cut as shown in Fig. 1a (i) and folded according to Fig. 1b. A double-faced adhesive tape with a punched hole of 8 mm in diameter was attached on the adsorption zone and then 10 mg of activated carbon impregnated with KOH was filled into the hole (ii). The purpose of the tape was to keep the carbon powder in place as well as to provide mechanical stability by forming a container for it. Next, the other side of adsorption paper zone was folded onto the side of activated carbon (iii). After assembly of the adsorption compartment, 10 μL aliquot of a 10 mmol L^{-1} Cu(II)-acetate solution in phosphate buffer (0.1 M, pH 6) was dropped directly onto the working electrode and dried at room temperature (iv). To accomplish the gPAD, the adsorption paper zone was folded onto the detection zone attaching it with an 8 mm punched double-faced adhesive tape (v) (Fig. 1b). Fig. 1c shows an exploded view of the gPAD. After fabrication, the gPADs were stored in a plastic tube containing N_2 gas.

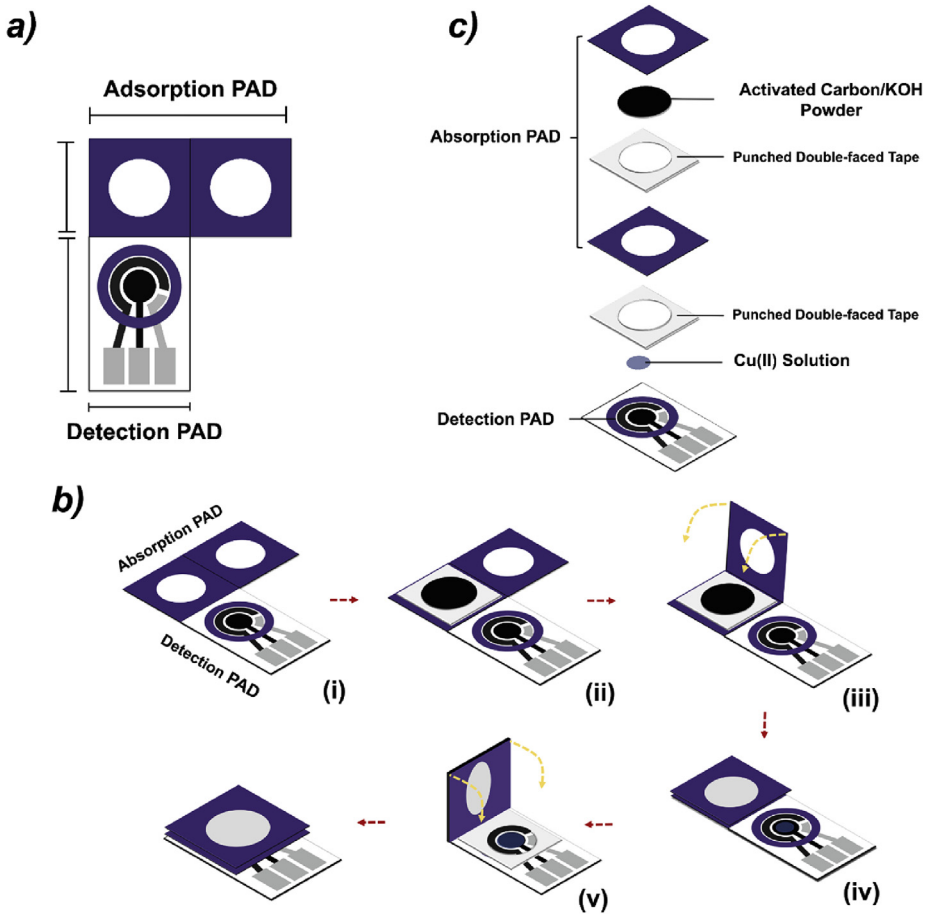

Fig. 1. Fabrication of the gPAD; (a) design of the origami device (blue zones indicate wax-impregnated areas); (b) fabrication started with cutting out the paper and printing (i), followed by attachment of the punched double-sided adhesive tape and filling with carbon (ii) and accomplishment of the adsorber by folding the paper (iii, iv); finally the adsorber was fixed to the sensing unit (v); (c) exploded view of the sensor. (For interpretation of the references to color in this figure legend, the reader is referred to the Web version of this article.)

2.5. NOx adsorption studies

Investigations were made in a static gas detection system, which was an air-tight box (volume 18 L), equipped with a computer cooling fan for easy gas mixing, a septum (1.5 cm in diameter) for injecting gases, and an inlet and an outlet (normally sealed with a silicon stopper to prevent gas exchange with the ambient air) to facilitate sampling of the total volume inside the box (Fig. S3, supplementary material). The sensors were placed on the bottom of the receptacle before closing it. The box was either filled with nitrogen for studies with NO, or with air for investigations with NO_2. Defined volumes of NO or other gases for interference studies were introduces with syringes through the septum. Except ozone, interfering gases were taken from corresponding steel cylinders, filled into glass flasks (2 L) and sealed with a septum through which required volumes were taken with a syringe.

Studies with ozone were done by generating ozone in a separate box (total volume 18 L) which was equipped with a septum, an in- and outlet, a corona discharge ozonizer (ATWFS, model Au-003-yg, purchased from www.amazon.de), and a computer cooling fan to generate ozone-containing atmospheres. The ozone concentration was quantified with standard potassium iodide titration. Corresponding volumes of ozone-containing air were sampled and added to the static gas detection system for interference studies.

2.6. Electrode modification and electrochemical measurements

The gPADs were placed in the static gas detecting system, as shown in Fig. S3 (supplementary material). Then, an NO gas standard was injected. In this step, NO_x gas was absorbed on the activated carbon in the adsorption paper zone for 25 min. After removal of the sensors from the chamber, 100 µL of phosphate buffer (0.1 M, pH 6) which acted as eluent and as supporting electrolyte at the same time were dropped onto adsorption paper zone which consequently passed through the activated carbon, eluted the adsorbed NO_2 (due to handling in air, adsorbed NO was converted to NO_2) and covered the three electrodes. The ensuing electrochemical procedure consisted of two steps: electrode modification and oxidation of follow-up products of NO_2. For the former, a potential of −1.2 V vs Ag/AgCl was applied for 60 s during which CuNPs were grown on the SPGE. During this process nitrate as a follow up product of NOx was reduced to nitrite. After modification and equilibration for 2 s, differential pulse voltammograms were recorded between 0.2 V and 1.3 V vs. Ag/AgCl with a scan rate of 20 mVs^{-1}, a pulse amplitude of 25 mV, a pulse rate 0.5 s and a pulse width of 60 ms. Current signals were evaluated as maximum peak heights.

2.7. Sample preparation

Indoor and outdoor air was collected at the Karl-Franzens University in Graz. The open chamber was exposed to the air for 5 min and then the gPADs were placed in it before closing. Likely, exhaust gases from cars were passed through the chamber via inlet and outlet for 2 min. The exposure time for the sensors was 25 min.

For comparative measurements with spectrophotometry, gas samples from the chamber were passed through 10 mL of absorbing reagent (11% v/v triethanolamine, 3.6% v/v ethylene glycol and 25% acetone in water) from which 1 mL was added to 4 mL of the Griess-Saltzman reagent (0.1% m:m NED, 1% m:m sulfanilamide in 5% v:v phosphoric acid). The concentration of NO_2 gas in the sample was evaluated using UV–Visible spectrophotometry at 540 nm and calibration curves (Passaretti Filho et al., 2015).

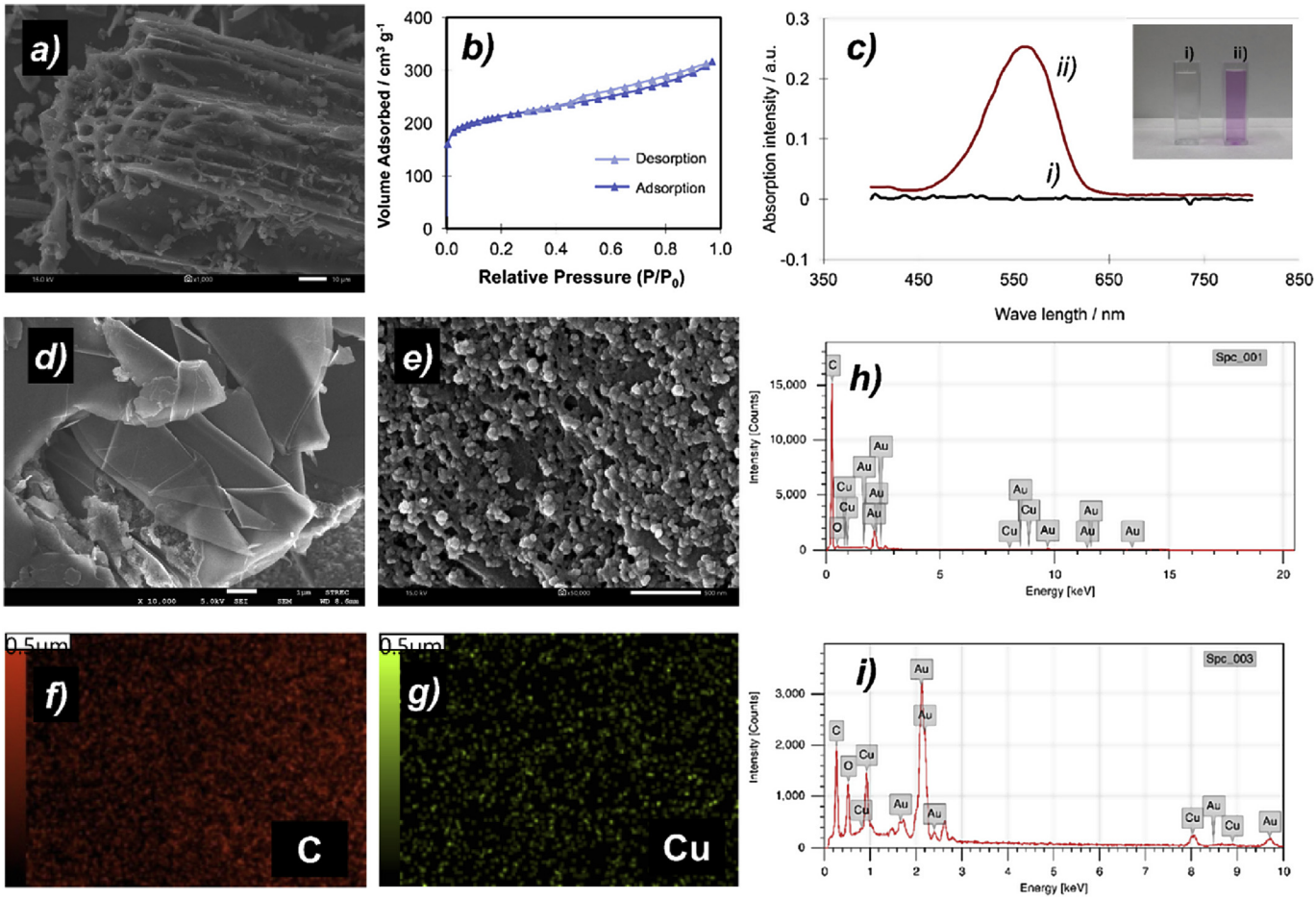

Fig. 2. Characterization of the adsorption layer (a–c), a bare SPGE (d, h) and a CuNP/SPGE (e, f, g, i): SEM images of activated carbon treated with KOH solution (a), a bare SPGE (d), a CuNP/SPGE (e); element mapping of carbon (f) and copper (g) of a CuNP/SPGE; Griess-Saltzman solution (b) after elution from activated carbon without (i) and with (ii) adsorbed NO_2 with corresponding UV-VIS absorption spectra (c); EDS spectra of a bare SPGE (h) and a CuNP/SPGE (i). Micrographs: the length of the white bar corresponds to the following lengths: 10 µm (a), 1 µm (d), 500 nm (e, f, g); the gradient bars of the element maps (f,g) designate practically pure carbon as light red and pure copper as light green. (For interpretation of the references to color in this figure legend, the reader is referred to the Web version of this article.)

3. Results and discussion

3.1. Morphological characterization of the adsorption layer and the working electrode

The surface morphologies of activated carbon packed in the adsorption PAD were investigated using scanning electron spectroscopy (SEM) as shown in Fig. 2a,d-g. The properties of activated carbon treated with KOH were investigated using surface area and pore size analysis. Nitrogen adsorption and desorption isotherms of activated carbon treated with KOH are shown in Fig. 2b. The pore size distribution was calculated from the data using the Brunauer-Joyner-Halenda (BJH) model. The mean pore diameter was found to be 2.46 nm indicating that activated carbon treated with KOH presents micro-porous structure. The BET (Brunauer-Emmett-Teller) surface area and total pore volume were calculated to be 798 $m^2 g^{-1}$ and 0.490 $cm^3 g^{-1}$ respectively. The results correspond very well with the findings of Lee et al. (2003). Activated carbon in the gPAD treated with KOH solution has high capacity for NO_2 adsorption due to the high surface area and the micro-porous structure.

To confirm adsorption of NO_2 on the surface of the activated carbon, a Griess-Saltzman solution was passed through the adsorption layer of the PAD in the absence and in the presence of adsorbed NO_2 (Fig. 2c inset). The presence of NO_2 is proven by the pink color of the solution due to the diazotization reaction. Fig. 2c displays the corresponding absorption spectra with a typical absorption maximum of the diazo compound at 540 nm. The results underline that the activated carbon impregnated in KOH can adsorb NO_2 gas.

The adsorption mechanism of NOx on KOH-activated carbon was studied by Lee et al. who found that potassium hydroxide is included in the carbon structure along with increased microporosity (Lee et al., 2003). Identified reaction products were potassium nitrite and nitrate. Beside NOx the modified carbon material showed good affinity for SO_2.

The surface morphologies of the bare SPGE and the CuNP/SPGE were also investigated by SEM. Successful modification with CuNPs on the SPGE was confirmed as shown in Fig. 2(d–i) that presents SEM images of the SPGE (d) and CuNP/SPGE (e) at 10,000X and 50,000× magnification, respectively. Clearly, there are significant differences in surface structure between the SPGE and the CuNP/SPGE. The bare SPGE has a smooth area of graphene sheets whereas the SEM image of a CuNP/SPGE shows that the spherical copper nanoparticles are dispersed on the SPGE surface with an average size of 59 nm in diameter. Moreover, energy dispersive X-ray spectra (EDS) manifested the presence of copper nanoparticles (Fig. 2 h, i) along with element mapping for carbon and copper (Fig. 2 f, g).

3.2. Electrochemical response of NOx at the gPAD

Cyclic voltammetry was performed to study the electrochemical behavior of NO_2 at a bare SPGE and a CuNP/SPGE as working

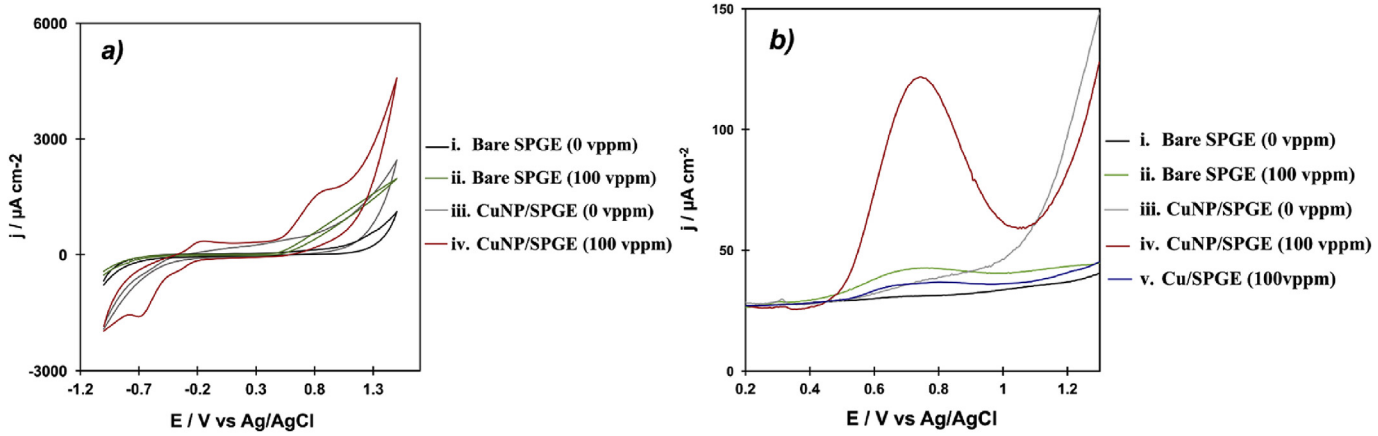

Fig. 3. Representative CVs (a) and DPVs (b) of different electrodes in the absence (i, ii) and presence (ii, iv, v) of NO_2; bare SPGE (i, ii), CuNP/SPGE (iii, iv) and Cu/SPGE (v). NO_2 concentration (i, iii, v): 100 vppm; experimental conditions: PBS (0.1 M, pH 6); conditioning time at −1.2 V: 60 s (i, ii, iii, iv), 0 s (v) and exposure time 25 min; electrode area 0.126 cm^2.

electrodes on gPADs. Fig. 3a shows cyclic voltammograms in the absence (i,iii) and presence of 100 vppm NO_2 in 0.1 M PBS pH 6 (ii, iv) recorded from −1.0 V to 1.5 V vs. Ag/AgCl on a bare SPGE(i, ii) and a CuNP/SPGE (iii,iv). No anodic peak was observable with 100 vppm NO_2 at a bare SPGE. However, anodic and cathodic peaks of NO_2 were found at 0.8 V and −0.7 V vs Ag/AgCl with a CuNP/SPGE.

In comparison to a bare SPGE, the peak currents of NO_2 at a CuNP/SPGE were higher due to the catalytic process of copper nanoparticles. To confirm the better performance of a CuNP/SPGE, differential pulse voltammograms of NO_2 were compared. A small signal at +0.75 V vs Ag/AgCl appears with the bare graphene electrode, which is enormously enhanced (around 9.6 times). in the presence of copper. Obviously the reduction of copper at negative potentials, forming catalytically active Cu(0) nanoparticles, co-reduces NO_2 or one of its follow-up products (nitrate) to a form which is easily oxidized at positive potentials, most probably nitrite (Kuang et al., 2018). Hence, these results demonstrate that the determination of NO_2 using a CuNP/SPGE coupled with activated carbon as adsorber yields a high-performance sensor, suggesting that the resulting gPAD can be an excellent device for NOx determination in the field.

An aim of this study was to uncover if NO and NO_2 behave similarly at the gPAD with respect to their adsorption behavior on activated carbon. NO in N_2 gas also was tested using the sensor under optimal condition (Fig. S4, supplementary material). The DPV responses did not show any significant difference of both species (± 5% relative error) neither alone or in combination. Thus, it may be concluded that gas sensing of NOx can be successfully achieved with the gPAD.

Thus, we may conclude that during adsorption potassium nitrite and nitrate are formed, from which the latter is reduced to electrochemically active nitrite by the catalytic action of copper nanoparticles during conditioning at −1.2 V vs Ag/AgCl. During electrochemical detection nitrite is oxidized to nitrate.

3.3. Optimization

All the experimental parameters, i.e., conditioning time and potential, concentration of the copper solution, pH of the supporting electrolyte as well as exposure time for high concentrations were optimized (Fig. S5, supplementary material) yielding the following values: conditioning time 60 s, conditioning potential −1.2 V, concentration of the copper solution 10 mM, pH of the supporting electrolyte 6, and exposure time for high concentrations (up to 100 vppm) 25 min.

Fig. 4 shows the adsorption isotherms for two low concentrations of NO_2, i.e., 0.5 and 1.0 vppm. Increasing the time yields increasing signals up to about 60 min; with longer periods the effect levels off

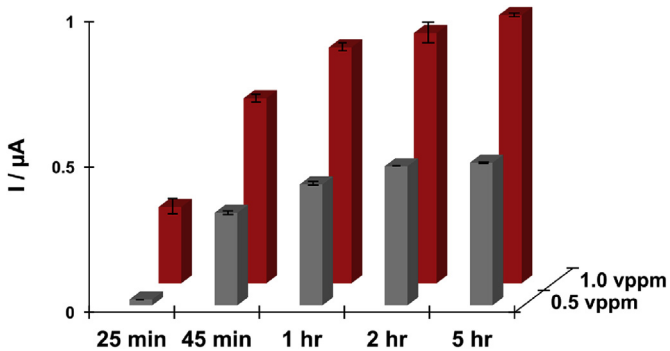

Fig. 4. Effect of exposure time on the signal of 0.5 and 1.0 vppm NO_2; signals (n = 3) shown as measured values (electrode area = 0.126 cm^2); other experimental parameters as in Fig. 3.

significantly. Thus, with concentrations higher than 1 vppm 25 min seem still proper for quantitative determinations with respect to reasonable analysis time. For lower concentrations, an exposure time of 1 h should be applied.

3.4. Analytical performance of the gPAD

Fig. 5 shows the dependence of the DPV current on the concentration of NO_2 (as NO in air) with an exposure time of 25 min. A linear relation between signal and concentration was obtained up to 150 vppm (a) with a linearity regression equation of I (µA) = 0.0907 C_{NOx} (vppm) + 0.0614 (R^2 = 0.99724), as shown in the inset. Above 150 vppm the signal started to level off. The limit of detection (LOD: $3\sigma/s$) and limit of quantitation (LOQ: $10\sigma/s$) was calculated to be 0.23 vppm and 0.76 vppm respectively. The LOD of the gPAD with 25 min exposure can be conveniently used to determine NO_x level in exhaust gases from cars for which a limit of 200 vppm has been set by EPA. The reproducibility in terms of relative standard deviation for the gPAD (n = 7 sensors; 25, 75 and 125 vppm NO_2) were found to be less than 5.1%.

With an exposure time of 60 min a dynamic range up to 5.0 vppm was determined with a regression equation (R^2 > 0.99), as shown in inset of Fig. 5b. The corresponding LOD was estimated as low as 0.03 vppm ($3\sigma/s$), the corresponding LOQ as 0.09 vppm. Hence, gPADs are able to detect maximum allowable NOx-levels in ambient air which EPA have set to 0.1 vppm. In addition, there was no obvious change in the current signal (less than ±10% of current signal) of 100 vppm NO_2 after storage for 30 days, as shown in Fig. S6 (supplementary material). Thus,

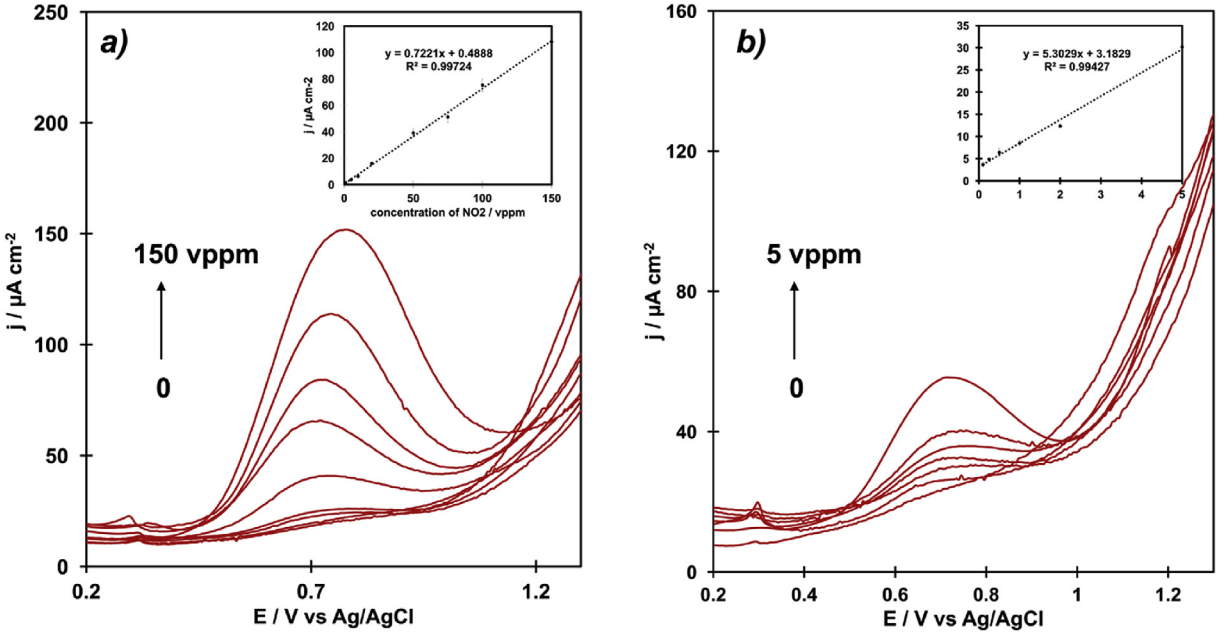

Fig. 5. Dependence of the DPV current at gPADs on the concentration of NOx with an exposure time of 25 (a) and 60 min (b). The insets show the calibration lines. Other experimental conditions as in Fig. 4.

gPADs can be used for over 30 days with the same response as at the beginning.

The results demonstrate that the NOx species are adsorbed strongly at the carbon and that the handling time (transfer of the sensors, connection to the instrument, application of the desorbing liquid) has no or only negligible influence on their desorption which is easily explainable by the formation of stable sorption products, such as potassium nitrite and nitrate.

3.5. Interferences

For interference studies gases were chosen which can occur in air samples and which were suspected that they might have an influence on the NOx determination. Ozone was included as a potential noxious trace component which can be formed by natural (photochemistry, electrical discharges) or anthropogenic processes. Nitrous oxide was considered as well as it can be released during denitrification by bacterial activity.

To air standards containing 50 vppm NO_x possibly interfering gases were added in defined volume ratios (given as $v_{interferent}$:v_{NOx}) to see their influence on the analytical signal (Fig. 6). The results show that 100-fold volume ratios of CO and of N_2O as well as a 50-fold ratio of SO_2 changed the signal only within the experimental error. Significant influence was observed with ozone, where the tolerable ratio was 0.5. A ratio of 1 (50 vppm ozone, 50 vppm NOx) caused a decrease of the signal of around 40% already.

Therefore, the developed sensor can be applied in real sample analysis without serious interferences of other common gases except in the presence of high concentrations of ozone.

3.6. Application to samples

The gPAD was used to determine NOx gas in three types of gas samples, namely ambient indoor and outdoor air, and exhaust gases from a diesel car. For the air samples 25 and 60 min adsorption time was applied, but no electrochemical signals could be observed in both cases. Comparative spectrophotometric measurements confirmed that the concentrations were below 0.03 vppm. Spiking with NO standards at levels of 1, 75 and 125 vppm yielded recoveries within an acceptable range from 95.9% and 105.1% (Table S1, supplementary material). Exhaust gases from a car were collected in a sealed box, in which gPADs were exposed for 25 min. The results showed levels of NOx from 67.0 to 124.6 vppm with an RSD of less than 4.2% which compared well with spectrophotometric determinations. A paired *t*-test of the results from the two methods uncovered that there was no significant statistical difference on a 95% confidence level because the calculated t-value (0.825) was lower than the critical value for two-tailed comparison (2.228). Thus, the gPAD presented here demonstrated high performance and high reliability for the determination of NOx in real samples.

4. Conclusion

A novel gas-sensing paper-based analytical device for the determination of NOx is presented. It shows a good potential for simple applications in the field due to low detection limits, reasonable analysis times and good tolerance towards SO_2, CO and N_2O. Moreover, the gPADs presented here are environmentally friendly, disposable, portable and low in production cost. The price for individual fabrication is significantly less than 1 USD per piece and can be still substantially lowered by mass production. As the sensor is designed as a one-shot sensor for single use only, no regeneration of the sensor surface is necessary. The gPAD for NOx determination presented here exhibits high sensitivity and selectivity applicable to environmental gas samples. In addition, it can be expected that similar devices for other gaseous analytes will be developed in the near future where this gPAD may serve as a template.

CRediT authorship contribution statement

Kingkan Pungjunun: Conceptualization, Investigation, Writing - original draft. **Sudkate Chaiyo:** Conceptualization, Visualization. **Narong Praphairaksit:** Validation. **Weena Siangproh:** Formal analysis. **Astrid Ortner:** Methodology. **Kurt Kalcher:** Project administration, Writing - review & editing. **Orawon Chailapakul:** Project administration, Funding acquisition. **Eda Mehmeti:** Supervision, Writing - review & editing.

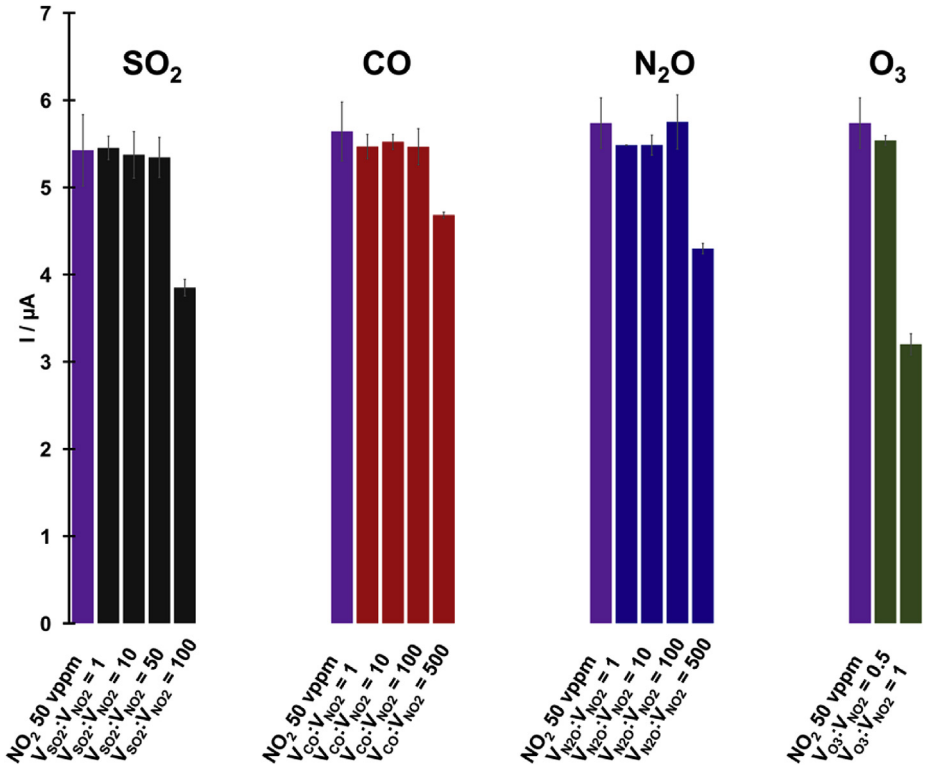

Fig. 6. Influence of trace gases on the sensor signal of NOx (50 vppm); ratios are given as v(interferent):v(NOx); the signals are shown as means of the measured values (n = 3).

Declaration of competing interest

The authors declare that they have no known competing financial interests or personal relationships that could have appeared to influence the work reported in this paper.

Acknowledgments

We would like to acknowledge support from the Science Achievement Scholarship of Thailand (SAST), the Overseas Research Experience Scholarship for Graduate Students: Chulalongkorn University, the Ratchapiseksompot Endowment Fund, and the Thailand Research Fund via the Research Team Promotion Grant (RTA6080002). Financial support from the ASEAN European Academic University Network (ASEA-UNINET) is highly appreciated (project ASEA 2019_Uni_Graz_1)

Appendix A. Supplementary data

Supplementary data to this article can be found online at https://doi.org/10.1016/j.bios.2019.111606.

References

Allen, C., Carrico, C.M., Gomez, S.L., Andersen, P.C., Turnipseed, A.A., Williford, C.J., Birks, J.W., Salisbury, D., Carrion, R., Gates, D., Macias, F., Rahn, T., Aiken, A.C., Dubey, M.K., 2018. JAPCA J. Air Waste Manag. 68 (11), 1175–1189.
Arduini, F., Cinti, S., Caratelli, V., Amendola, L., Palleschi, G., Moscone, D., 2019. Biosens. Bioelectron. 126, 346–354.
Belhachemi, M., Jeguirim, M., Limousy, L., Addoun, F., 2014. Chem. Eng. J. 253, 121–129.
Brown, M.D., Schoenfisch, M.H., 2018. Electrochim. Acta 273, 98–104.
Chaiyo, S., Mehmeti, E., Siangproh, W., Hoang, T.L., Nguyen, H.P., Chailapakul, O., Kalcher, K., 2018. Biosens. Bioelectron. 102, 113–120.
Deng, S., Tjoa, V., Fan, H.M., Tan, H.R., Sayle, D.C., Olivo, M., Mhaisalkar, S., Wei, J., Sow, C.H., 2012. J. Am. Chem. Soc. 134 (10), 4905–4917.
Dumitrescu, E., Wallace, K.N., Andreescu, S., 2018. Nitric Oxide 74, 32–38.
Dungchai, W., Chailapakul, O., Henry, C.S., 2009. Anal. Chem. 81 (14), 5821–5826.
Ghouma, I., Jeguirim, M., Dorge, S., Limousy, L., Matei Ghimbeu, C., Ouederni, A., 2015. Cr. Chim. 18 (1), 63–74.
Gomes, F.O., Maia, L.B., Loureiro, J.A., Pereira, M.C., Delerue-Matos, C., Moura, I., Moura, J.J.G., Morais, S., 2019. Bioelectrochemistry 127, 76–86.
Hoa, N.D., El-Safty, S.A., 2011. Chem. Eur J. 17 (46), 12896–12901.
Izumi, K., Utiyama, M., Maruo, Y.Y., 2015. Sens. Actuators B Chem. 216, 128–133.
Jeong, H.-S., Park, M.-J., Kwon, S.-H., Joo, H.-J., Kwon, H.-I., 2019. Sens. Actuators B Chem. 288, 625–633.
Jung, J., Lee, J., Kim, B., Oh, S., 2017. Atmos. Environ. 165, 290–300.
Kuang, P., Natsui, K., Einaga, Y., 2018. Chemosphere 210, 524–530.
Lee, Y.-W., Kim, H.-J., Park, J.-W., Choi, B.-U., Choi, D.-K., Park, J.-W., 2003. Carbon 41 (10), 1881–1888.
Lu, L., 2019. Sens. Actuators B Chem. 281, 182–190.
Ma, C., Li, W., Kong, Q., Yang, H., Bian, Z., Song, X., Yu, J., Yan, M., 2015. Biosens. Bioelectron. 63, 7–13.
Manoj, D., Saravanan, R., Santhanalakshmi, J., Agarwal, S., Gupta, V.K., Boukherroub, R., 2018. Sens. Actuators B Chem. 266, 873–882.
Moreira, C.M., Pereira, S.V., Raba, J., Bertolino, F.A., Messina, G.A., 2018. Clin. Chim. Acta 486, 59–65.
Nantaphol, S., Kava, A.A., Channon, R.B., Kondo, T., Siangproh, W., Chailapakul, O., Henry, C.S., 2019. Anal. Chim. Acta 1056, 88–95.
Panraksa, Y., Siangproh, W., Khampieng, T., Chailapakul, O., Apilux, A., 2018. Talanta 178, 1017–1023.
Passaretti Filho, J., da Silveira Petruci, J.F., Cardoso, A.A., 2015. Talanta 140, 73–80.
Prakash, S., Rajesh, S., Singh, S.K., Bhargava, K., Ilavazhagan, G., Vasu, V., Karunakaran, C., 2011. Talanta 85 (2), 964–969.
Pungjunun, K., Chaiyo, S., Jantrahong, I., Nantaphol, S., Siangproh, W., Chailapakul, O., 2018. Microchim. Acta. 185 (7).
Rajesh, N., Kannan, J.C., Leonardi, S.G., Neri, G., Krishnakumar, T., 2014. J. Alloy. Comd 607, 54–60.
Rattanarat, P., Dungchai, W., Cate, D., Volckens, J., Chailapakul, O., Henry, C.S., 2014. Anal. Chem. 86 (7), 3555–3562.
Song, Y., Chen, F., Zhang, Y., Zhang, S., Liu, F., Sun, P., Yan, X., Lu, G., 2019.
Sun, X., Li, B., Tian, C., Yu, F., Zhou, N., Zhan, Y., Chen, L., 2018. Anal. Chim. Acta 1007, 33–39.
Suryaraman, M.G., Viswanathan, A., 1949. J. Chem. Educ. 26 (11) 594.
Thornton, J.A., Wooldridge, P.J., Cohen, R.C., 2000. Anal. Chem. 72 (3), 528–539.
Zhang, J., Ma, J., Zhang, S., Wang, W., Chen, Z., 2015. Sens. Actuators B Chem. 211, 385–391.